Microscopic Structure in a Shpol'skii System: A Single-Molecule Study of Dibenzanthanthrene in *n*-Tetradecane

Andreas Bloess, Yannig Durand, Michio Matsushita, Rogier Verberk, Edgar J. J. Groenen,* and Jan Schmidt*

Centre for the Study of Excited States of Molecules, Huygens Laboratory, Leiden University, P.O. Box 9504, 2300 RA Leiden, The Netherlands

Received: August 8, 2000; In Final Form: January 4, 2001

A study is presented of the orientation of single 2.3, 8.9-dibenzanthanthrene molecules in *n*-tetradecane as a function of their spatial position on a length scale of 2 mm down to a few hundreds of nanometers at 1.4 K, which allows us to obtain structural information about this host/guest system. In the confocal detection volume of $\sim 10\ \mu m^3$ the guest molecules show two preferential orientations. A broad distribution of orientations of about $\pm 17^\circ$ is observed around these two mean orientations. The mean orientations exhibit long-range order even over a distance of 2 mm with gradual variations on a micrometer scale. Over distances smaller than the lateral dimension of the confocal detection volume these variations disappear almost completely whereas the widths of the distributions remain qualitatively the same. The results do not point to the presence of a polycrystalline structure which contradicts the common picture of Shpol'skii systems.

Introduction

When quickly frozen, host/guest systems of *n*-alkanes and aromatic hydrocarbons may show a drastic narrowing of the electronic transitions of the embedded hydrocarbons. This so-called Shpol'skii effect was first reported in 1952.[1] The reduction of the line width of more than 1 order of magnitude, compared to what is commonly observed in glassy hosts, indicates a considerable decrease in the spread of interaction strengths between the embedded chromophore and the surrounding matrix. This spread is determined by the strength of the coupling between chromophore and environment in combination with the amount of disorder in the host/guest system. The occurrence of narrow Shpol'skii lines, often superimposed on a broad background, is thought to result from a partial crystallization of the *n*-alkane during the fast cooling process. A fraction of the guest molecules may end up in an ordered environment. For these molecules the large degree of freedom present in a glassy matrix is drastically reduced and therefore the optical transitions of the ensemble are narrowed. The degree of line narrowing has been shown to depend on the rate of cooling, the concentration of the guest molecules, and the length of the *n*-alkane chain.

Besides the considerable decrease in line width, the presence of so-called multiplet, fine, or site structure is well-known for Shpol'skii spectra.[2−4] When one compares the spectra of the same guest molecule in a quickly frozen *n*-alkane and in a slowly grown single crystal of the same *n*-alkane, only minor differences are observed in the multiplet structure.[5] This suggests that the observed multiplicity of the electronic transitions is not a result of the fast cooling process but that it is intrinsic to the given host/guest combination. In the literature the presence of multiplets is discussed in terms of different crystal structures in the rapidly solidified *n*-alkane matrix,[6] the presence of rotational isomers of the *n*-alkane molecules next to their most stable form,[2,3] and different ways the impurity molecules are incorporated into the matrix leading to distinct orientations of the guest molecules in the crystal lattice.[7] The latter hypothesis has been confirmed by polarization studies in absorption and luminescence,[8−10] EPR,[5] ODMR,[11] and Zeeman[12] experiments carried out on slowly grown samples for particular host/guest combinations.

The present picture of the microscopic structure of Shpol'skii matrixes is based on bulk measurements. Meanwhile, single-molecule studies have been found feasible for several hydrocarbons in *n*-alkane matrixes.[13−20] In particular, in the work of Irngartinger[21] the orientation of individual terrylene guest molecules in a frozen *n*-hexadecane matrix was determined by polarization-dependent measurements. In an attempt to shed light on the microscopic structure of Shpol'skii matrixes, we have started a systematic study of the orientation of individual dibenzanthanthrene (DBATT) molecules as a function of their spatial position in a quickly frozen *n*-tetradecane matrix. The orientation of the DBATT guest molecules was measured on a scale from 2 mm down to a few hundred nanometers. This investigation of the orientation of the DBATT impurity molecules on a single-molecule level provides structural information on the incorporation of the guest molecules, which has so far been difficult to obtain for mixed-crystal systems. Within the confocal detection volume the guest molecules show preferential orientations as in a single crystal, but there is a broad distribution of orientations around the two observed mean orientations. While the two mean orientations of the DBATT molecules reveal long-range order on distances as large as 2 mm with gradual variations that are further and further reduced from millimeter distances to submicrometer distances, the widths of the distributions of orientations around the two mean orientations remain qualitatively the same. These results contradict the common picture of polycrystallinity of Shpol'skii systems.

Experimental Section

A single-mode dye laser (Coherent, 899-21, Rhodamine 6G), with a bandwidth smaller than 1 MHz, provides the excitation light around 600 nm. The output of the laser is stabilized in intensity by an electrooptical modulator (EOM, ConOptics) and

* Corresponding authors. Fax: +31-71-5275819. E-mail: mat@molphys.leidenuniv.nl.

10.1021/jp002863k CCC: $20.00
Published on Web 03/06/2001

directed via a polarization preserving single-mode fiber to the microscope. The absolute frequency of the laser is obtained by recording the excitation spectrum of iodine. Inside the cryostat an aspheric single lens (Thorlabs, $f = 1.45$ mm, NA $= 0.55$) is used to collect the fluorescence signal from the sample and, in the confocal case, also to focus the excitation beam. In the configuration with this single objective lens, a long-pass cutoff filter (Omega EFLP 610), and an avalanche photodiode (APD, EG&G SPCM-AQ-161), the fluorescence photons are detected with an overall efficiency of (0.2 ± 0.1)%. Alternatively, the signal could be recorded with an image-intensified CCD camera (Princeton Instruments Pentamax GenIV).

In the polarization studies of the orientation of the dopant molecules over spatial ranges of 2 mm and 70 μm, the microscope was used in a back-illumination configuration. A Berek polarization compensator (New Focus model 5540) was used as a half-wave plate to turn the polarization of the excitation light. An area of about 100 μm in diameter was illuminated. The collected fluorescence was selected by two long-pass cutoff filters (Omega EFLP 610, Omega EFLP 620).

In the experiment with subdiffraction-limited resolution the microscope was used in a confocal configuration.[22] The confocal principle led to a reduction of the background light intensity by a factor of about 5, which is essential to achieve a spatial resolution beyond the diffraction limit. In the polarization study with the confocal configuration a liquid-crystal variable retarder (Newport, model 932 C) in combination with a quarter-wave plate was used as an electronically driven half-wave plate. A short-pass filter was added to the excitation path to cut off red fluorescence from the fiber. The fluorescence was selected again by the same long-pass cutoff filters and directed either onto the APD or onto the APD and the CCD camera simultaneously.

The sample position could be adjusted mechanically in a horizontal plane, either perpendicular to or along the optical axis, with an accuracy of about 1 μm. Photon counts from the APD were read by a multichannel scaling card (EG&G 923 MCS-plus) configured for continuous circularly buffered counting. The whole experiment was controlled and processed through a computerized data acquisition system.[23]

The sample was prepared by dissolving 2.3, 8.9-dibenzanthanthrene (DBATT) in *n*-tetradecane. DBATT was purchased from Dr. W. Schmidt (PAH Research Institute, 86926 Greifenberg, Germany), and *n*-tetradecane 99%, from Acros Organics. After 3 h in an ultrasonic bath, the solution with an estimated concentration of 10^{-6} mol/L was brought onto a circular LiF substrate (10 mm in diameter) and covered with a 100 μm thin quartz plate. All preparation steps were done in the dark or in red light to prevent as much as possible the photooxidation of DBATT. The insertion of the sample holder into the precooled (liquid nitrogen) cryostat resulted in a frozen film about 20 μm thick. The experiments were carried out at (1.4 ± 0.2) K with the sample immersed in liquid helium.

An important aspect to be considered when analyzing polarization-dependent data is the possible misinterpretation due to birefringence of the sample. We have tested various samples to select one with negligible birefringence. For the sample used in the studies reported here, the linear polarization of incident laser light (at 514 and 632 nm), after passing through the sample, was turned by less than $\pm 5°$ and the linearity of the polarization remained better than 92% for all spatial positions investigated.

Results and Discussion

Figure 1 shows characteristic images of different samples, obtained in transmission with light of a tungsten lamp which illuminated the sample from the backside in a standard microscope configuration. Dark areas in the images indicate sample regions of low transmission and bright areas those of high transmission. Seen from outside the cryostat, all samples had the same milky appearance, but although we kept the preparation conditions as constant as possible, the magnified images in Figure 1 reveal strong differences between different samples. There are diffuse structures with little order (Figure 1a) and nicely arranged mosaic-like structures with bright areas separated by dark boundaries (Figure 1b,c). The transmission in the dark areas is typically 60−80% less than in the bright areas. All measurements, on which we report in the following, were carried out on the sample, part of which is shown in Figure 1a.

Ensemble fluorescence-excitation spectra of DBATT in *n*-tetradecane, obtained with a laser with a bandwidth of about 1 wavenumber, are shown in Figure 2. The spectrum in Figure 2a was obtained by probing a volume of a few hundred μm^3. This was achieved by moving the sample to an out-of-focus position in the detection as well as in the back-illumination light path. Figure 2b,c presents typical ensemble spectra of molecules in the confocal detection volume of ~ 10 μm^3. All spectra show a substantial background. The lines at 16 967 and 17 037 cm^{-1} are assigned to two 0−0 transitions, and the smaller peaks at 17 212 and 17 282 cm^{-1}, to vibronic replicas. Statistical fine structure (SFS) is clearly visible on the 0−0 transitions in Figure 2b,c, which reflects the decreased spectral density of molecules in the small detection volume. This SFS is less pronounced on the vibronic bands because of the shorter lifetime of the vibronic states. The 0−0 transitions in Figure 2a show a fwhm of 22 and 16 cm^{-1}. These are typical values for line widths observed in bulk measurements of similar Shpol'skii systems.[13,15,17,18,20,24] For a bulk sample of DBATT in *n*-hexadecane a line width of about 15 cm^{-1} is reported.[16] The line width observed in our sample remains the same when reducing the volume to 10 μm^3. We conclude that the energetic disorder within macroscopic volumes of Shpol'skii systems is still present in volumes as small as some cubic micrometers.

The detection volume (indicated by white circular dots in Figure 1a), which is smaller than the structures in the white-light images, allowed us to look for changes in the spectra when going from bright to dark areas. The spectrum in Figure 2b belongs to a spatial position that is dark in the white-light transmission image whereas the spectrum in Figure 2c belongs to a position that is bright. No noticeable differences are observed. At all probed positions, the spectra show the two excitation lines with essentially the same line width, and no correlation was observed between the signal-to-background ratio and the structures in the white-light images. This holds as well for samples exhibiting mosaic-like structures. The ensemble experiments provide no indication that the mosaic-like structure derives from microcrystalline domains separated by glassy ribbons. We interpret the structures in the white light images as irregularities such as cracks that are formed during the cooling process to release the strain in the material. The same interpretation is given by Irngartinger et al.,[25] who observed in the white light images an ongoing formation of structures during the cooling process of a sample of terrylene in *n*-hexadecane even at temperatures far below the freezing point of *n*-hexadecane.

To shed more light on the microstructure, we have studied the orientation of individual DBATT molecules incorporated in the *n*-tetradecane matrix. The 0−0 transitions of individual DBATT molecules were resolved throughout the two 0−0 bands by reducing the excitation bandwidth by about 4 orders of

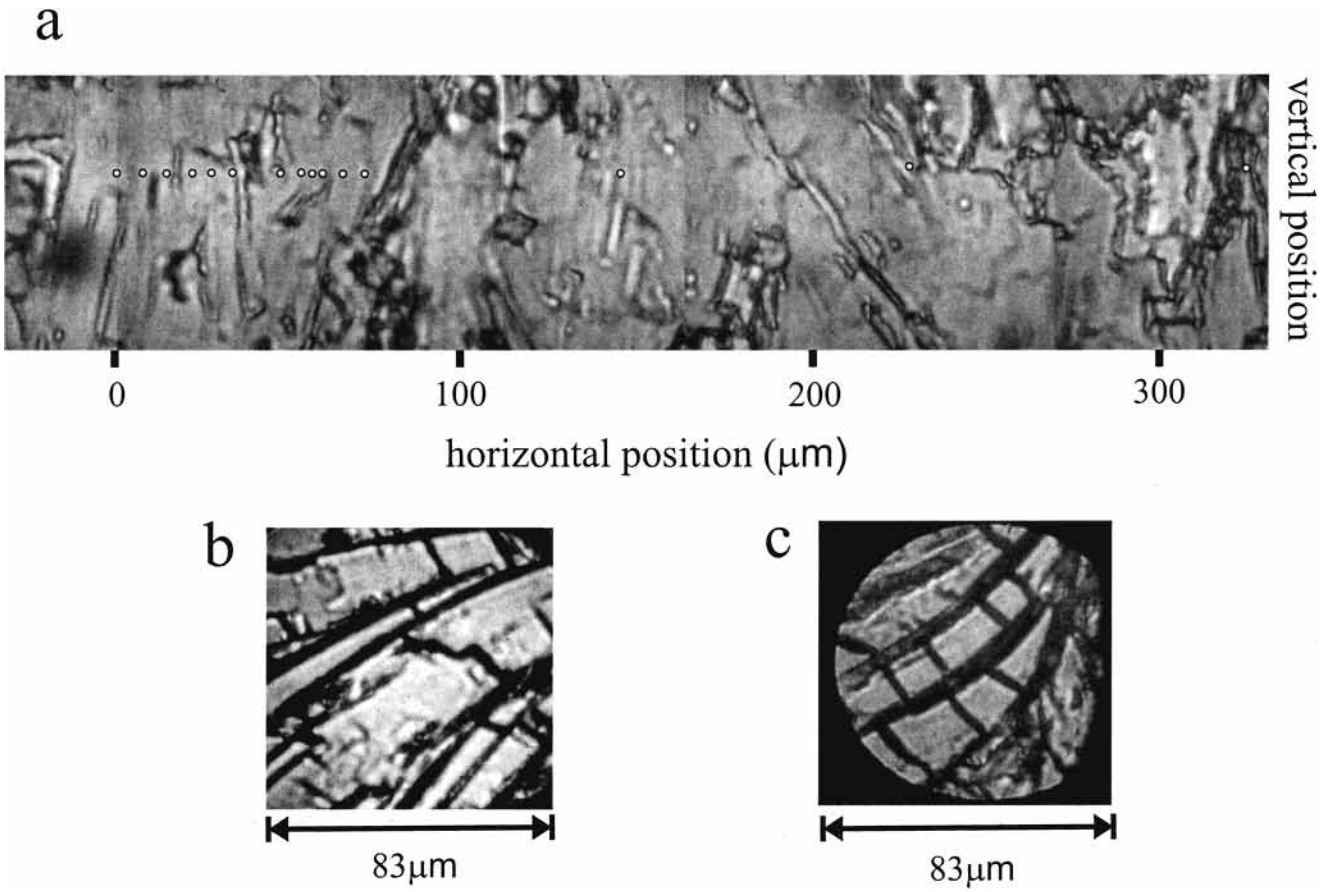

Figure 1. White-light transmission images of different samples of a frozen solution of DBATT dissolved in *n*-tetradecane at 1.4 K. (a) shows a combination of seven transmission images with the white dots indicating the size and the position of some of the probed volumes. The circular field of view in (c) is due to the detection aperture, which was smaller in that case.

magnitude. Figure 3a shows an example of a scan over 6 GHz with the frequency presented along the vertical direction. Each horizontal trace in this intensity graph represents the dependence of the fluorescence of a single molecule on the polarization of the excitation light. The maxima within a trace refer to the orientation of the transition dipole moment of the corresponding molecule projected onto the lateral plane (for convenience we refer to this direction as "the orientation of the molecule" throughout the paper). In the experiments, the linear polarization of the excitation light was turned from 0 to 360° in steps of 10°. The fluorescence was detected without any polarization selectivity. For each angle 3−5 frequency sweeps were recorded, separated by a sweep during which the excitation light was blocked and the orientation of the half-wave plate was changed manually. A histogram representing the orientations of molecules selected within the two 0−0 bands at a given spatial position is presented in Figure 3b. It reveals that there are two main orientations of the guest molecules corresponding to two preferred incorporations into the matrix. We will refer to the distribution of orientations centered around 170° as site 1 and the distribution centered around 60° as site 2.

Figure 4a shows the mean orientation and the width of the distribution of orientations of the DBATT molecules from site 1 and site 2 as a function of the position of the focus on a horizontal line in the sample (as indicated by the white dots in Figure 1a) over a distance of 2 mm in steps of about 150 μm. At each spatial position we spectrally selected on average 97 molecules. The mean orientation and the width (two times the standard deviation) are determined from histograms such as that in Figure 3b. Subsequently, the experiment was repeated on a shorter length scale, over a distance of 70 μm in steps of 6 μm. The result is presented in Figure 4b. Most noteworthy, Figure 4a,b shows that the average orientation of molecules does not change randomly in the sample. We observe a long-range order of the embedded guest molecules over distances of 70 μm and even 2 mm. The variation of the mean orientation over a distance of 2 mm is 50° for site 1 and 80° for site 2. On the micometer-length scale the mean orientations are gradually changing. Besides the observation of two distinct orientations, a relatively wide variation of molecular orientations (average width of 34°), already within the detection volume of $\sim$10 μm^3, is observed for both sites. This is considerably more than observed for pentacene in the single crystal *p*-terphenyl, for which a width of 6−8° has been reported.[26] The widths of the orientation distributions of the two sites vary over the sample between 20 and 60°. These observations do not point to the presence of crystal domains larger than the confocal detection volume.

In the next step, the spatial resolution has been increased even further. The orientation of the DBATT molecules was studied on a scale smaller than a micrometer, within the detection volume, as a function of their spatial positions. The required spatial resolution that surpasses the limit imposed by the setup was achieved by applying an optical superresolution technique,[22] which takes advantage of the frequency selectability of the guest molecules owing to the inhomogeneous broadening in the ensemble spectrum. By combination of this technique with polarization measurements, the lateral coordinates of the individual molecules were obtained with subdiffraction-limited accuracy together with the orientation of the molecules. The measurements within the confocal detection volume were performed at an arbitrary position in the frozen sample, and a total of 314 DBATT molecules were selected around the centers

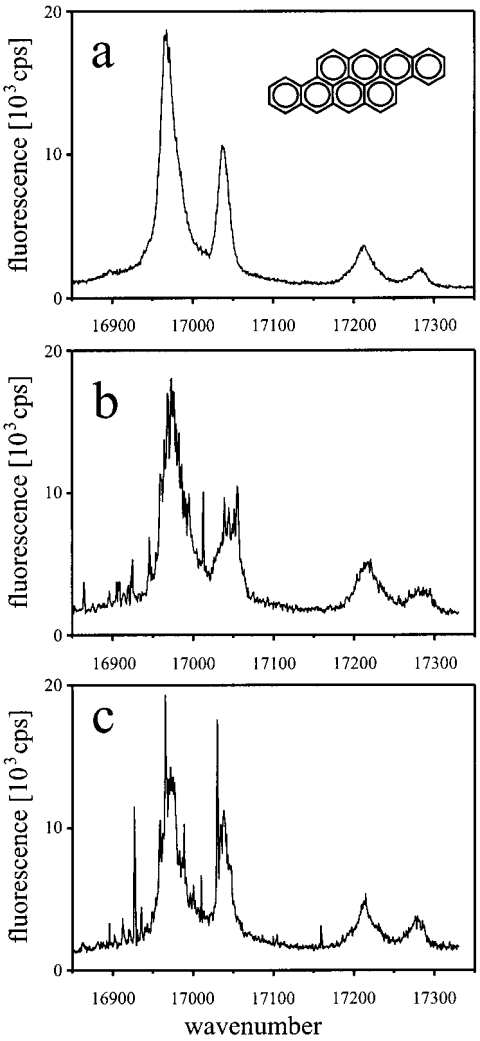

Figure 2. Broad-band fluorescence-excitation spectra of DBATT in *n*-tetradecane from molecules in a volume larger than the confocal detection volume (a) and from molecules within the confocal detection volume (b, c) for sample positions which were bright (b) and dark (c) in the white-light transmission images. The molecular structure of DBATT is given as an inset in (a).

of the two 0−0 transitions. Regions of 20 GHz, separated by 1 wavenumber, were chosen successively. For each 20 GHz range first the orientation of 10−30 individual molecules was determined by recording spectra similar to the one presented in Figure 3a. From the fluorescence intensity as a function of polarization, and taking into account the polarization characteristics of the half-wave retardation device and the beam-splitter, the orientation of these individual molecules was found within a mean error of ±3.6°. In a second step, the lateral coordinates of the 10−30 molecules observed in each 20 GHz scan were determined by slowly scanning the laser (1 GHz/20 s) and recording the fluorescence simultaneously with the APD and the CCD camera. The camera was taking 1 picture/s. When the laser was in resonance with a single molecule, this resulted in a peak in the spectrum recorded by the APD and at the same time in a two-dimensional photon distribution on the CCD camera. An evaluation of the center of the photon distribution yields the lateral position of the molecule. The accuracy in this position is determined by the long-term stability of the whole setup, the error due to the finite number of collected photons of each individual molecule, and the background noise. The long-term stability is found to be 19 nm for a total measuring time of 9 h. The average error due to the finite number of collected photons

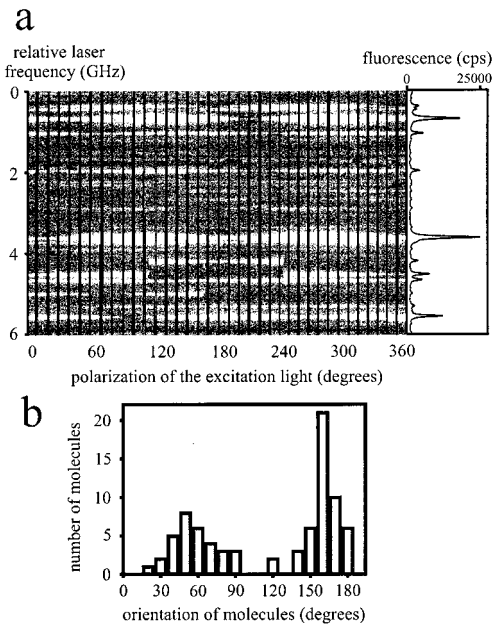

Figure 3. (a) Excitation spectra (excitation frequency along the vertical axis) as a function of the polarization of the excitation light (horizontal axis) together with the average spectrum over all sweeps. (b) A histogram of the orientations of single molecules obtained from traces such as the one shown in (a).

is 12 nm, and the average error due to the background noise 2 nm. A total average accuracy of the lateral positions of 23 nm (in terms of the standard deviation) results. By comparison of the spectrum taken with the APD during the measurement of the spatial position with the corresponding spectrum measured in the polarization studies, the proper orientation was assigned to the molecules. The axial coordinate of the molecules was not determined. To measure these would have required considerably more time thus reducing the number of molecules studied by roughly a factor of 10.

The results of the superresolution experiment are summarized in Figures 5 and 4c. The histogram in Figure 5a shows the distribution of the orientations of the 314 molecules selected within the confocal detection volume. In the center of the first 0−0 line about two molecules were detected per GHz. Orientation and lateral coordinates have been determined for half of the detected molecules. The 314 molecules represent roughly 10% of all molecules present within the confocal detection volume. The two main distributions for this particular spatial position show a width of 26° (site 1) and 30° (site 2) which are typical for the distributions shown in Figure 4a,b. The mean orientations are 176 and 81° for sites 1 and 2, respectively. The lateral positions and orientations of the molecules from sites 1 (186 molecules) and 2 (128 molecules) are shown in Figure 5b,c. The orientations are indicated by sticks, and the circles represent the error in the position of the individual molecules. Molecules of the two sites are distributed randomly inside the detected volume. There is no evidence for a spatial separation of the two sites. In Figure 4c the mean values and the widths of the orientation distributions of six subensembles of the 314 DBATT molecules are presented as a function of their spatial position. The subensembles were selected by binning the molecules along the horizontal coordinate. A comparison of the widths in Figures 4c and 5a shows no narrowing of the distribution of orientations within subvolumes of the confocal detection volume. Inspection of Figure 4a−c shows that the variation in the mean orientations of the guest molecules is reduced when going from distances of millimeters to distances

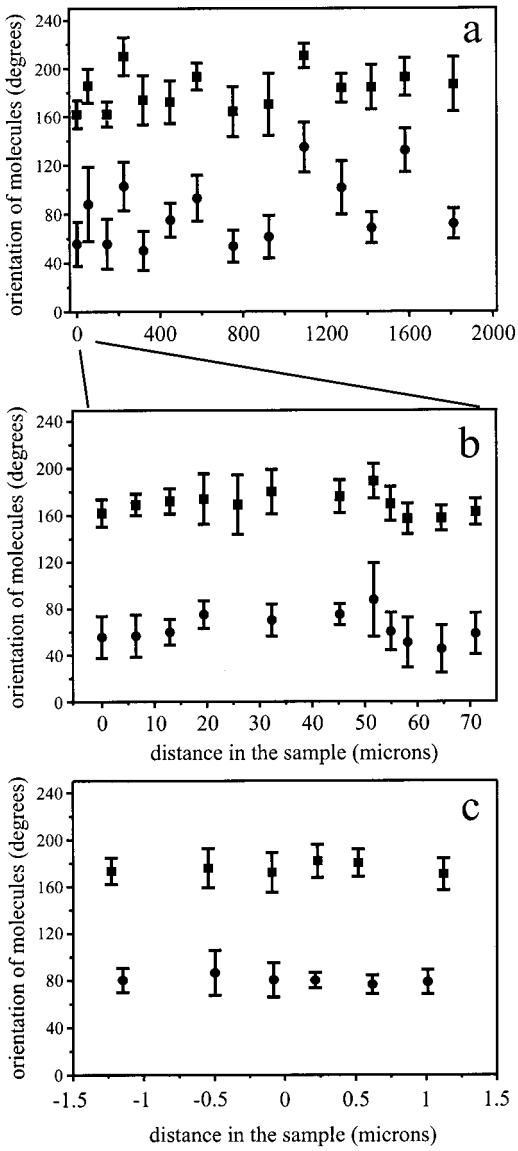

Figure 4. Spatial dependence of the mean value (squares and circles) and the width (bars) of the distribution of the orientations of DBATT molecules within the confocal detection volume in the frozen *n*-tetradecane host. The orientation behavior is followed for molecules from site 1 (squares) and site 2 (circles) over a distance of 2 mm (a), 70 μm (b), and 2 μm (c). A total number of 1361 (a), 1153 (b), and 314 single molecules (c) is represented. The data shown in (c) are from the same molecules as presented in Figure 5. Each point in (c) represents a subensemble of 31 (squares) or 21 (circles) molecules. The subensembles were selected by binning the molecules along the horizontal coordinate.

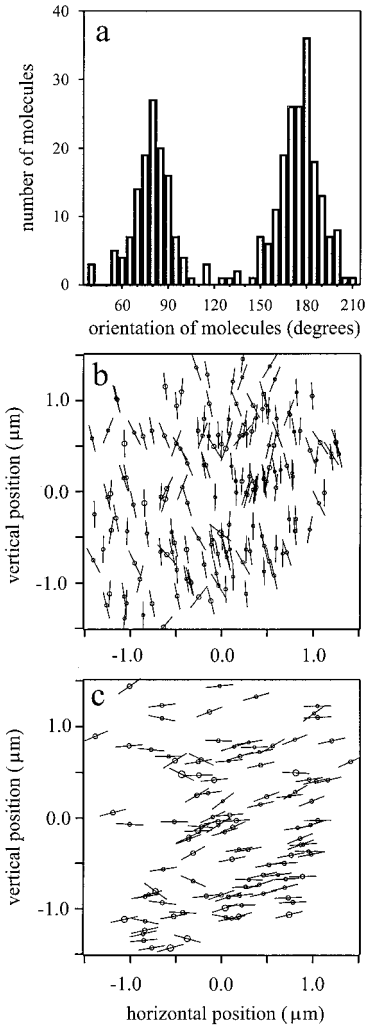

Figure 5. (a) Histogram of the orientations of all 314 DBATT guest molecules selected within the confocal detection volume of $\sim$10 μm^3. (b) Position and orientation of 186 DBATT molecules of site 1 in the frozen *n*-tetradecane host. (c) The same for 128 molecules from site 2. The lateral positions are indicated by circles and the orientations by sticks. The size of the circles indicates the error in the lateral positions of the individual molecules.

of a few hundred nanometers whereas the width in the distribution remains qualitatively the same at all length scales. In particular there is no indication of the presence of crystallites with dimensions of hundreds of nanometers.

Conclusion

The analysis of the ensemble spectra in relation to the white-light transmission images does not reveal a correlation between the sometimes observed mosaic-like structures and the line width, the line intensity, or the signal-to-background ratio in the excitation spectra. The tempting interpretation of the bright areas as crystalline domains and the dark areas as domain boundaries consisting of less-ordered, glassy material is not sustained by our experiments.

In the orientation studies of single DBATT molecules in a quickly frozen matrix of *n*-tetradecane the presence of two main orientations of the guest molecules in the host matrix is found. There is a considerable width of 20−60° in the distribution of orientations around the mean values. The two mean orientations of DBATT molecules within the confocal detection volume of $\sim$10 μm^3 show long-range order even over a distance of 2 mm. The mean orientations vary gradually with position, and the variation becomes less going from the milimeter distance to the tens of micrometers scale. On the micrometer scale these variations have almost disappeared. On the other hand, the widths of the orientation distributions qualitatively remain unchanged. Even within subvolumes of the confocal detection volume no narrowing of the distribution of orientations is found. We conclude that the observed width in the distributions of orientations is intrinsic to the Shpol'skii system. The sample is neither polycrystalline nor single crystalline. The preferred orientations on a micrometer scale and the long-range order reminds one of a crystalline morphology, but the orientations reveal a broad distribution and do gradually change with position. In our case, down to dimensions of several hundreds

of nanometers the results do not point to the presence of crystalline domains.

The ensemble line width of DBATT in *n*-tetradecane of about 20 cm^{-1} and the width in the distribution of the orientations, both being larger than typical values found for aromatic hydrocarbons in single-crystal hosts, might suggest a correlation between the resonance frequency of the embedded guest molecules and their orientation. In this respect subtle effects have been observed and will be discussed in a forthcoming paper.

Acknowledgment. This work is part of the research program of the "Stichting voor Fundamenteel Onderzoek der Materie" (FOM) and has been made possible by financial support from the "Nederlandse Organisatie voor Wetenschappelijk Onderzoek" (NWO).

References and Notes

(1) Shpol'skii, É. V.; Il'ina, A. A.; Klimova, L. A. *Dokl. Akad. Nauk SSSR* **1952**, *87*, 935.

(2) Shpol'skii, É. V. *Usp. Fiz. Nauk* **1960**, *71*, 215; *Sov. Phys. Usp*. **1960**, *3*, 372.

(3) Shpol'skii, É. V. *Usp. Fiz. Nauk* **1962**, *77*, 321; *Sov. Phys. Usp*. **1962**, *5*, 522.

(4) Shpol'skii, É. V. *Usp. Fiz. Nauk* **1963**, *80*, 255; [*Sov. Phys. Usp*. **1963**, *6*, 411.

(5) Lamotte, M.; Merle, A. M.; Joussot-Dubien, J.; Dupuy, F. *Chem. Phys. Lett*. **1975**, *35*, 410.

(6) Miosya, E. G. *Opt. Spektrosk*. **1967**, *23*, 119; *Opt. Spectrosc*. **1967**, *23*, 220.

(7) Bowen, E. J.; Brocklehurst, B. *J. Chem. Soc.* **1955**, *4*, 4320.

(8) Malykhina, N. N.; Sphak, M. T. *Opt. Spektrosk*. **1963**, *14*, 829; *Opt. Spectrosc*. **1963**, *14*, 442.

(9) Personov, R. I.; Bykovskaya, L. A. *Dokl. Akad. Nauk SSSR* **1971**, *199*, 299; *Sov. Phys. Dokl*. **1972**, *16*, 556.

(10) Gorbachev, S. M.; Zalesskii, I. E.; Nizhnikov, V. V. *Opt. Spektrosk.* **1983**, *54*, 482; *Opt. Spectrosc. (USSR)* **1983**, *54*, 284.

(11) Merle, A. M.; Pitts, W. M.; El-Sayed, M. A. *Chem. Phys. Lett*. **1978**, *54*, 211.

(12) Jansen, G.; Noort, M.; van Dijk, N.; van der Waals, J. H. *Mol. Phys*. **1980**, *39*, 865.

(13) Moerner, W. E.; Plakhotnik, T.; Irngartinger, T.; Croci, M.; Palm, V.; Wild, U. P. *J. Phys. Chem*. **1994**, *98*, 7382.

(14) Plakhotnik, T.; Walser, D.; Pirotta, M.; Renn, A.; Wild, U. P. *Science* **1996**, *271*, 1703.

(15) Pirotta, M.; Renn, A.; Werts, M. H. V.; Wild, U. P. *Chem. Phys. Lett*. **1996**, *250*, 576.

(16) Boiron, A.-M.; Lounis, B.; Orrit, M. *J. Chem. Phys*. **1996**, *105*, 3969.

(17) Vacha, M.; Tani, T. *J. Phys. Chem. A* **1997**, *101*, 5027.

(18) Vacha, M.; Liu, Y.; Nakatsuka, H.; Tani, T. *J. Chem. Phys*. **1997**, *106*, 8324.

(19) Mais, S.; Tittel, J.; Basché, Th.; Bräuchle, C.; Göhde, W.; Fuchs, H.; Müller, G.; Müllen, K. *J. Phys. Chem. A* **1997**, *101*, 8435.

(20) Durand, Y.; Bloess, A.; van Oijen, A. M.; Köhler, J.; Groenen, E. J. J.; Schmidt, J. *Chem. Phys. Lett*. **2000**, *317*, 232.

(21) Irngartinger, T. H. A. Abbildende Einzelmolekül-Spektroskopie von Terrylene. Thesis, Zürich, 1997; Chapter 4.6.

(22) Oijen van, A. M.; Köhler, J.; Schmidt, J.; Müller, M.; Brakenhoff, G. J. *J. Opt. Soc. Am. A* **1999**, *16*, 909.

(23) Brouwer, A. C. J. Optical and magnetic-resonance spectroscopy on single molecules. Thesis, Leiden, 1999; Chapter 5.

(24) Palewska, K.; Lipinski, J.; Sworakowski, J.; Sepiol, J.; Gygax, H.; Meister, E. C.; Wild, U. P. *J. Phys. Chem*. **1995**, *99*, 16835.

(25) Irngartinger, T.; Renn, A.; Zumofen, G.; Wild, U. P. *J. Lumin*. **1998**, *76*−*77*, 279.

(26) Güttler, F.; Croci, M.; Renn, A.; Wild, U. P. *Chem. Phys*. **1996**, *211*, 421.